High-Temperature Leakage Improvement in Metal–Insulator–Metal Capacitors by Work–Function Tuning

K. C. Chiang, C. H. Cheng, H. C. Pan, C. N. Hsiao, C. P. Chou, Albert Chin, *Senior Member, IEEE*, and H. L. Hwang, *Fellow, IEEE*

***Abstract*—Using low-cost and high work–function Ni, a low leakage current of 5×10^{-6} A/cm^2 at 125 °C is obtained in a high 25-fF/μm^2-density $SrTiO_3$ metal–insulator–metal (MIM) capacitor processed at 400 °C. This is approximately two orders of magnitude better than the same device using a TaN electrode, with added advantages of improved voltage and temperature coefficients of capacitance. This work–function tuning method also has merit for achieving both low thermal leakage and high overall κ value beyond previous laminate structure.**

***Index Terms*—Capacitor, high temperature, metal–insulator–metal (MIM), Ni, thermal leakage.**

I. Introduction

As THE VERY large scale integration (VLSI) scaling continues, the thermal effect on IC becomes a serious issue due to the increasing integration density, large power density, and high chip temperature. This becomes even worse by the large dc leakage and power consumption from ultrathin gate oxides. Such leakage current at elevated temperature is especially important for advanced charge-storage MIM capacitors [1]–[14], where the smaller conduction band offset (ΔE_C) in higher κ dielectric [15] further degrades the thermal leakage but is needed for the required higher capacitance density. To address this issue, an Al_2O_3-HfO_2 laminate structure [8] is used, and a high ΔE_C Al_2O_3 is used to decrease the thermal leakage. However, the improved high-temperature leakage current is traded off with the capacitance density and κ value. To overcome the above problems, in this letter, we have used work–function (ϕ_m) tuning to improve the thermal leakage without scarifying overall κ in MIM devices. The near two orders lower leakage current at 125 °C are obtained using low-cost and high-ϕ_m Ni (5.1 eV) on high-κ $SrTiO_3$ than control TaN (4.5 eV). Using the Ni electrode also has the merit of much lower cost than the expensive and rare Noble metals [11]. The measured 125-°C leakage of 5×10^{-6} A/cm^2 at 25-fF/μm^2 capacitance density is also one of the lowest reported data without trading off the high-κ value [1]–[14], with added merits of improved voltage and temperature coefficients of capacitance (VCC and TCC) needed for the analog/RF application.

Manuscript received December 6, 2006. This work was supported in part by Technology Development Program of Academia (TDPA) Department of Industrial Technology (DOIT) Ministry of Economic Affairs (MOEA) under Grant 94-EC-17-A-01-S1-047 and National Science Council (NSC) under Grant 95-2221-E-009-275 of Taiwan. The review of this letter was arranged by Editor A. Wang.

K. C. Chiang and A. Chin are with the Department of Electronics Engineering, National Chiao-Tung University, Hsinchu 30010, Taiwan, R.O.C. (e-mail: albert_achin@hotmail.com).

C. H. Cheng and C. P. Chou are with the Department of Mechanical Engineering, National Chiao-Tung University, Hsinchu 30056, Taiwan, R.O.C.

H. C. Pan and C. N. Hsiao are with the Instrument Technology Research Center, National Applied Research Laboratories, Hsinchu 300, Taiwan, R.O.C.

H. L. Hwang is with the Department of Electrical Engineering, National Tsing-Hua University, Hsinchu 30013, Taiwan, R.O.C.

Color versions of one or more of the figures in this letter are available online at http://ieeexplore.ieee.org.

Digital Object Identifier 10.1109/LED.2007.891265

II. Experimental Procedure

The TaN/Ta bilayer metal was deposited on SiO_2/Si substrate by sputtering and patterned to form the bottom capacitor electrode. The TaN surface was further treated by NH_3 plasma nitridation [4], [10]–[14] to enhance the diffusion barrier property, which in turn improves oxygen deficiency and capacitance density by reducing the interfacial TaON formation during postdeposition anneal (PDA) [13], [14]. Then, 23- or 46-nm-thick $SrTiO_3$ dielectric layer was deposited using an RF magnetron sputter system with ceramic target, followed by the subsequent 400-°C furnace annealing for 1 h under oxygen ambient for dielectric quality improvement. This process temperature is lower than previous 450-°C-formed nanocrystal $SrTiO_3$ [13], [14] for better backend integration and improved device uniformity, although the overall κ value is lowered due to the mixed amorphous and crystalline phase. Finally, Ni, control TaN, or Al was deposited and patterned to form the top capacitor electrode, and the fabricated devices were characterized by capacitance–voltage (C–V) and density–voltage (J–V) measurements.

III. Results and Discussion

Fig. 1(a) and (b) shows the C–V and J–V characteristics of $SrTiO_3$ MIM capacitors with different Ni, TaN, or Al metal electrode, respectively. At $\sim$12-fF/μm^2 capacitance density, the device with a Ni electrode shows the desired less voltage and frequency dependences, which are related to the measured significant lower leakage current. The leakage current improvement increases greatly with increasing temperature to 125 °C due to the exponential temperature dependence, where more than two orders of magnitude lower leakage current are

0741-3106/$25.00 © 2007 IEEE

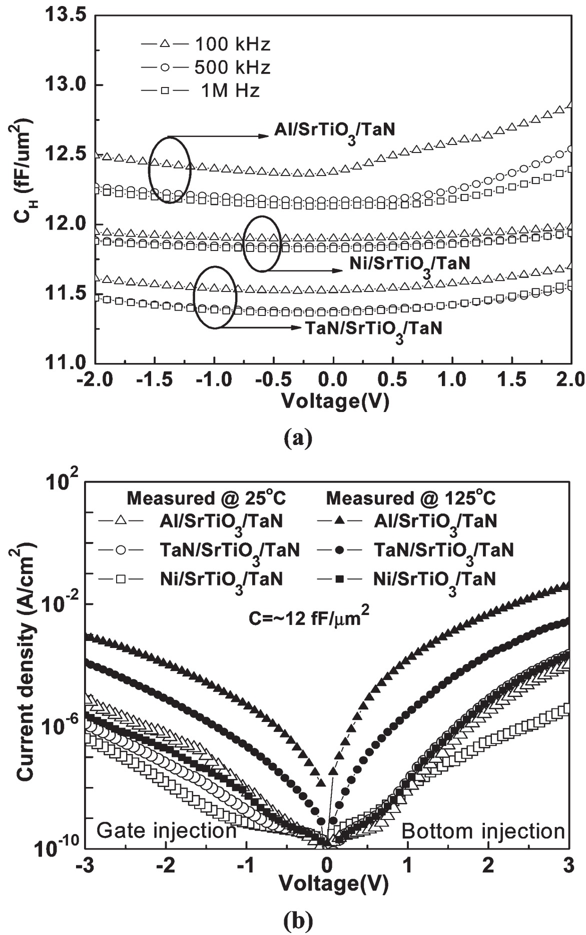

Fig. 1. (a) C–V and (b) J–V characteristics of $\sim$12-fF/μm^2 $SrTiO_3$ MIM capacitors with different Ni, TaN, or Al top electrode, respectively. Both the 25-°C and 125-°C J–V data are measured.

measured using Ni electrode than TaN. Furthermore, a high breakdown voltage and a field of 10 V and 2.2 MV/cm were measured for Ni electrode, which shows the good potential for real application.

The operation condition is less than the breakdown voltage and is investigated by the time-to-breakdown (t_{BD}) study. Fig. 2(a) shows the t_{BD} lifetime and stability of $SrTiO_3$ devices after a thermal treatment of 350 °C for 1 h. A still high field of 1.4 MV/cm for the extrapolated ten-year lifetime is obtained after thermal treatment, indicating the good reliability and process integration capability. In addition, we further studied the ϕ_m effect on higher density capacitor of 25 fF/μm^2. Fig. 2(b) shows the J–V characteristics of $SrTiO_3$ MIM capacitors with various metal electrodes. Similar remarkably large improvement of thermal leakage is obtained at 125 °C, where low current of only 5×10^{-6} A/cm^2 is measured at a 25-fF/μm^2 capacitor. This is one of the lowest reported thermal leakage currents at 25-fF/μm^2 density [1]–[14].

Fig. 3 shows the $\Delta C/C$–V characteristics of $SrTiO_3$ MIM capacitors with 12- or 25-fF/μm^2 density. Similar to the previous works [9]–[14], the quadratic VCC (α) improves with decreasing leakage current and capacitance density. At $\sim$12-fF/μm^2 density, low 125-°C leakage current of 2×10^{-7} A/cm^2 at 2 V, and small α of 392 ppm/V^2 are simulta-

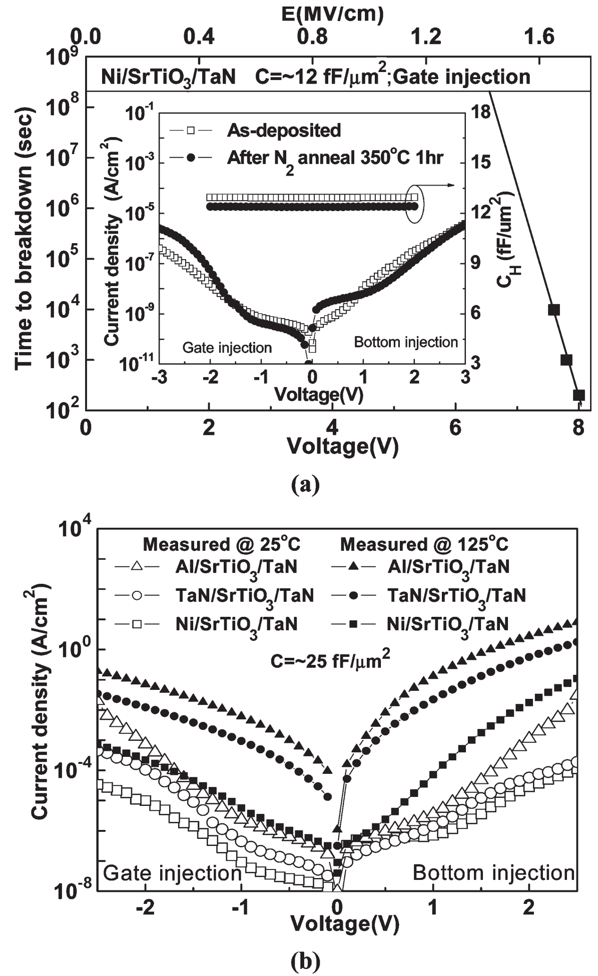

Fig. 2. (a) Time-to-breakdown lifetime and thermal stability test for Ni/$SrTiO_3$/TaN capacitor. (b) 25-°C and 125-°C measured J–V characteristics of $\sim$25-fF/μm^2 $SrTiO_3$ MIM capacitors with different Ni, TaN, or Al top electrode.

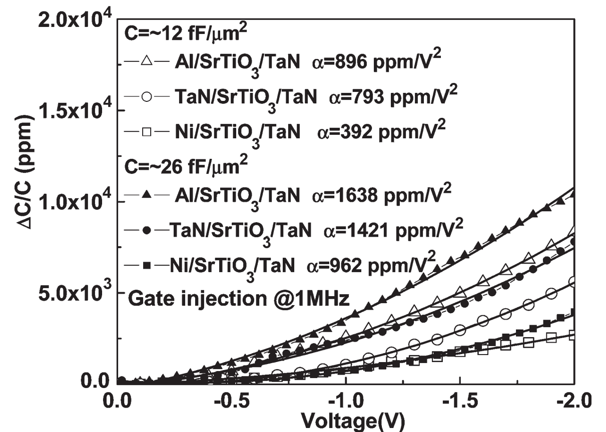

Fig. 3. $\Delta C/C$–V characteristics of $\sim$12- or $\sim$25-fF/μm^2 $SrTiO_3$ MIM capacitors with different Ni, TaN, or Al top electrode.

neously measured, which are comparable with or better than the best reported data in literature [1]–[14]. Similar improved TCC is also measured for $SrTiO_3$ MIM capacitors, where TCC of 804, 423, and 334 ppm/°C are measured for 12 fF/μm^2-density devices with Al, TaN, and Ni electrodes, respectively.

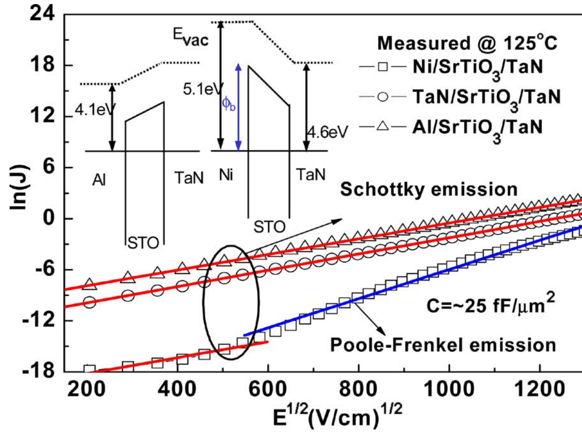

Fig. 4. Measured and calculated 125-°C J–$E^{1/2}$ characteristics of ∼25-fF/μm^2 $SrTiO_3$ MIM capacitors with different Ni, TaN, or Al top electrode. The inserted figure is the band diagrams under thermal equilibrium.

To investigate the large leakage current difference for $SrTiO_3$ MIM capacitors with various Ni, TaN, and Al electrodes, we have plotted $\ln(J)$ versus $E^{1/2}$ in Fig. 4. The measured data fit well with the calculation by either Schottky emission (SE) or Frenkel–Poole (FP) conduction as follows:

$$J \propto \exp\left(\frac{\gamma E^{1/2} - V_b}{kT}\right) \tag{1}$$

$$\gamma = \left(\frac{e^3}{\eta\pi\varepsilon_0 K_\infty}\right)^{1/2}. \tag{2}$$

The K_∞ is the high-frequency dielectric constant ($= n^2$, where n is the refractive index). The η is a constant with its value equal to 1 or 4 for FP or SE, respectively, which gives the slope γ to be 1.6×10^{-5} or 3.18×10^{-5} eV(m/V)$^{1/2}$ by applying $n = 2.4$ of $SrTiO_3$ [14], [16] into the previous equations. From the good agreements between measured and (1) calculated data, the 125-°C leakage current of $SrTiO_3$ devices with Al or TaN electrode is dominated by SE over the whole electric field due to small metal/insulator barrier height (ϕ_b). In sharp contrast, the leakage from Ni electrode is dominated by SE only at a low field but governed by a trap-conducted FP mechanism at a high field, which is due to a large ϕ_b, shown in the inserted thermal equilibrium-band diagram.

IV. Conclusion

Much improved thermal leakage current at 125 °C is obtained by using low-cost and high-ϕ_m Ni electrode in $SrTiO_3$ MIM capacitors fabricated at 400 °C for VLSI backend integration. The lower leakage also shows improved VCC and TCC and important for analog/RF ICs.

Acknowledgment

The authors from National Chiao-Tung University would like to thank Prof. H. Iwai's valuable discussion.

References

[1] C.-M. Hung, Y.-C. Ho, I.-C. Wu, and K. O, "High-Q capacitors implemented in a CMOS process for low-power wireless applications," in *Proc. IEEE MTT-S Int. Microw. Symp.*, 1998, pp. 505–511.

[2] J. A. Babcock, S. G. Balster, A. Pinto, C. Dirnecker, P. Steinmann, R. Jumpertz, and B. El-Kareh, "Analog characteristics of metal–insulator–metal capacitors using PECVD nitride dielectrics," *IEEE Electron Device Lett.*, vol. 22, no. 5, pp. 230–232, May 2001.

[3] Y. L. Tu, H. L. Lin, L. L. Chao, D. Wu, C. S. Tsai, C. Wang, C. F. Huang, C. H. Lin, and J. Sun, "Characterization and comparison of high-κ metal–insulator–metal (MIM) capacitors in 0.13 μm Cu BEOL for mixed-mode and RF applications," in *VLSI Symp. Tech. Dig.*, 2003, pp. 79–80.

[4] Y. K. Jeong, S. J. Won, D. K. Jwon, M. W. Song, W. H. Kim, O. H. Park, J. H. Jeong, H. S. Oh, H. K. Kang, and K. P. Suh, "High quality high-k MIM capacitors by $Ta_2O_5/HfO_2/Ta_2O_5$ multilayered dielectric and NH_3 plasma interface treatments for mixed-signal/RF applications," in *VLSI Symp. Tech. Dig.*, 2004, pp. 222–223.

[5] X. Yu, C. Zhu, H. Hu, A. Chin, M. F. Li, B. J. Cho, D.-L. Kwong, P. D. Foo, and M. B. Yu, "A high-density MIM capacitor (13 fF/μm^2) using ALD HfO_2 dielectrics," *IEEE Electron Device Lett.*, vol. 24, no. 2, pp. 63–65, Feb. 2003.

[6] S. J. Kim, B. J. Cho, M.-F. Li, C. Zhu, A. Chin, and D. L. Kwong, "HfO_2 and lanthanide-doped HfO_2 MIM capacitors for RF/mixed IC applications," in *VLSI Symp. Tech. Dig.*, 2003, pp. 77–78.

[7] C. Zhu, H. Hu, X. Yu, S. J. Kim, A. Chin, M. F. Li, B. J. Cho, and D. L. Kwong, "Voltage and temperature dependence of capacitance of high-κ HfO_2 MIM capacitors: A unified understanding and prediction," in *IEDM Tech. Dig.*, 2003, pp. 879–882.

[8] H. Hu, S. J. Ding, H. F. Lim, C. Zhu, M. F. Li, S. J. Kim, X. F. Yu, J. H. Chen, Y. F. Yong, B. J. Cho, D. S. H. Chan, S. C. Rustagi, M. B. Yu, C. H. Tung, A. Du, D. My, P. D. Fu, A. Chin, and D. L. Kwong, "High performance HfO_2-Al_2O_3 laminate MIM capacitors by ALD for RF and mixed signal IC applications," in *IEDM Tech. Dig.*, 2003, pp. 379–382.

[9] S. J. Kim, B. J. Cho, M. B. Yu, M.-F. Li, Y.-Z. Xiong, C. Zhu, A. Chin, and D. L. Kwong, "High capacitance density (>17 fF/μm^2) Nb_2O_5-based MIM capacitors for future RF IC applications," in *VLSI Symp. Tech. Dig.*, 2005, pp. 56–57.

[10] K. C. Chiang, A. Chin, C. H. Lai, W. J. Chen, C. F. Cheng, B. F. Hung, and C. C. Liao, "Very high-κ and high density TiTaO MIM capacitors for analog and RF applications," in *VLSI Symp. Tech. Dig.*, 2005, pp. 62–63.

[11] K. C. Chiang, C. C. Huang, A. Chin, W. J. Chen, S. P. McAlister, H. F. Chiu, J. R. Chen, and C. C. Chi, "High-κ Ir/TiTaO/TaN capacitors suitable for analog IC applications," *IEEE Electron Device Lett.*, vol. 26, no. 7, pp. 504–506, Jul. 2005.

[12] K. C. Chiang, C. H. Lai, A. Chin, T. J. Wang, H. F. Chiu, J. R. Chen, S. P. McAlister, and C. C. Chi, "Very high density (23 fF/μm^2) RF MIM capacitors using high-κ TiTaO as the dielectric," *IEEE Electron Device Lett.*, vol. 26, no. 10, pp. 728–730, Oct. 2005.

[13] K. C. Chiang, C. C. Huang, A. Chin, W. J. Chen, H. L. Kao, M. Hong, and J. Kwo, "High performance micro-crystallized TaN/$SrTiO_3$/TaN capacitors for analog and RF applications," in *VLSI Symp. Tech. Dig.*, 2006, pp. 126–127.

[14] K. C. Chiang, C. C. Huang, A. Chin, G. L. Chen, W. J. Chen, Y. H. Wu, A. Chin, and S. P. McAlister, "High performance $SrTiO_3$ metal–insulator–metal capacitors for analog applications," *IEEE Trans. Electron Devices*, vol. 53, no. 9, pp. 2312–2319, Sep. 2006.

[15] J. Robertson, "Band offsets of wide-band-gap oxides and implications for future electronic devices," *J. Vac. Sci. Technol. B, Microelectron.*, vol. 18, no. 3, pp. 1785–1791, May 2000.

[16] F. Gervais, *Handbook of Optical Constants of Solids II*, E. D. Palik, Ed. New York: Academic, 1991, p. 1035.